Micellization Kinetics in Block Copolymer Solutions: Scaling Model

Elena E. Dormidontova

Department of Polymer Chemistry and Material Science Centre, University of Groningen, Nijenborgh 4, 9747 AG Groningen, The Netherlands

Received June 8, 1998; Revised Manuscript Received July 12, 1999

ABSTRACT: The kinetics of micelle evolution of diblock copolymers from unimers toward the equilibrium state is studied analytically on the basis of consideration of the kinetic equations. The association/dissociation rate constants for unimer insertion/expulsion and micelle fusion/fission are calculated by applying Kramers' theory combined with a scaling approach. It is shown that the difference in the intermediate results and the rate of association for the "unimer exchange" mechanism and the joint "micelle fusion/fission + unimer exchange" mechanism is remarkable, with the latter being much more effective. According to this mechanism, at the beginning of the micellization, after coupling of free unimers is completed, fusion of micelles becomes dominant, whereas unimer exchange is effectively frozen by the high activation energy required for unimer release. The later stages of micelle evolution involve both unimer exchange and micelle fusion, which is considerably slowed with time as the average micelle size increases. Micelle fission is also a relatively slow process that however plays an important role in micelle reequilibration occurring with a decrease in the equilibrium aggregation number (as e.g., during T-jump experiments). Applications of the theory to experimental results are discussed in detail.

Introduction

Micellization kinetics in block copolymer solutions has attracted considerable interest during the past decade[1−16] with a number of recent papers.[6−16] Different experimental techniques such as the stopped-flow method,[1] temperature-jump experiments (T-jump), [8,12−14] nonradiative energy transfer and fluorescence-quenching techniques,[3,6,7] time-resolved light scattering,[8,12−14] transmission electron microscopy,[15,16] and sedimentation velocity methods for comicellization experiments[4,5] have been applied to obtain detailed information about the kinetics of micellar formation or reequilibration. Despite the extensive experimental data collected, a unified scenario of micellar evolution has not been presented. An analytical solution of this problem is attempted in the present paper by employing Kramers' theory and a scaling approach for calculation of association/dissociation rate constants appearing in kinetic equations. In addition, we discuss the applications of the scenario of micelle equilibration suggested by our theory to various experimental situations.

Up to the present time, experimental observations concerning relaxation kinetics in block copolymer solutions have been analyzed in terms of theoretical models describing micellization kinetics in surfactant systems.[17−21] Surfactant micelles differ in their structure and equilibrium properties from block copolymer micelles, so it is natural to expect that micellization kinetics in these polymer systems is different as well. Two main mechanisms of surfactant micelle evolution are distinguished. According to the unimer exchange mechanism, micelle growth occurs by the consecutive incorporation of unimers (schematically shown in Figure 1) according to the following equation:

$$N_{Q-1} + N_1 \rightleftharpoons N_Q \qquad (1)$$

where N_Q is the number density of micelles with aggregation number Q.

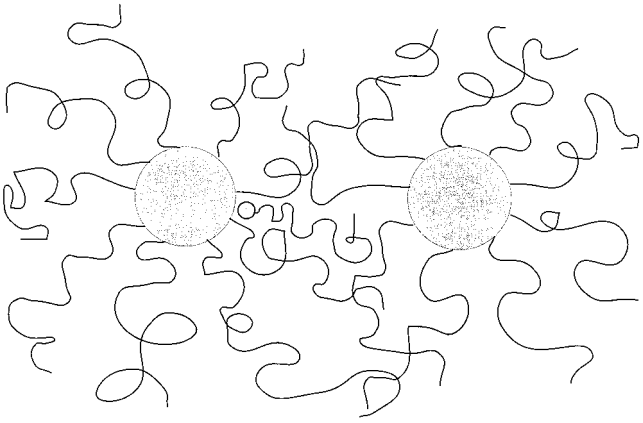

Figure 1. Schematic picture of unimer exchange.

Unimer exchange is a rather fast process with the corresponding relaxation time τ_{unim}:

$$\frac{1}{\tau_{unim}} \simeq \frac{k^-}{\sigma^2} + \frac{k^-}{Q} X(1 + C_o) \qquad (2)$$

where k^- is the unimer expulsion rate constant, Q is the average aggregation number of the micelles, σ is the width of the micellar size distribution, $X = (c - c_{un}/c_{un})$, is the relative fraction of micelles (compared to free unimers of concentration c_{un}), and C_o is the average relative concentration deviation from the equilibrium among the micelles.[17−19] This model of unimer exchange between surfactant micelles was proposed by Aniansson and Wall[17−19] for small deviations from the equilibrium state. The model implies that the number of micelles does not change during consecutive unimer association, though occasionally surfactant micelles can dissociate into unimers increasing the number of free unimers and hence, facilitating subsequent association.

According to the second mechanism of surfactant association, the evolution proceeds via micellar fusion/

10.1021/ma9809029 CCC: $18.00 © 1999 American Chemical Society
Published on Web 10/15/1999

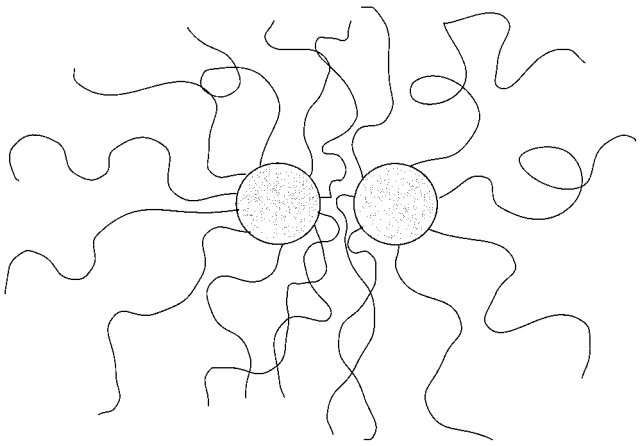

Figure 2. Schematic picture of micelle fusion/fission.

fission (shown schematically in Figure 2) described by the following equation:

$$N_{Q1} + N_{Q2} \rightleftarrows N_{Q1+Q2} \tag{3}$$

Micellar fusion/fission is considered to be responsible for the slowly relaxing component that is often observed

$$\frac{1}{\tau_{\text{fus}}} \simeq \beta \frac{\bar{Q}X}{1 + (\sigma^2/\bar{Q})X} \tag{4}$$

where β is a measure of the mean dissociation rate constant. Like the unimer exchange model, the model of micellar fusion/fission[20,21] is based on the assumption of small deviations from the equilibrium state, i.e., where there is a balance between association and dissociation processes.

Despite the superficial similarity between surfactant and block copolymer micelles, the latter differs considerably from the former in the structure of micellar core, where, instead of a surfactant's relatively short alkyl chain, long entangled polymer blocks are present. Hence, the expulsion rate constants for block copolymer chains must differ from those for surfactants. The corresponding analysis of the unimer expulsion rate constant for block copolymer micelles has been performed by Halperin and Alexander.[2] The main conclusion of their paper[2] is that unimer exchange is the only mechanism for block copolymer micelle evolution. It is necessary to note, however, the following: (i) The results obtained[2] are valid only for small deviations from the equilibrium state. (ii) The characteristic time for unimer expulsion is underestimated, because the unimer has to diffuse through the whole corona region (which is much larger than the size of a blob neighboring the core, $\xi(R_{\text{core}})$, as was considered by Halperin and Alexander[2]). In addition, the time for insoluble block disentanglement has not been taken into account, either. (iii) The association/dissociation rates for micellar fusion/fission have not been calculated. Therefore, any categorical conclusion about the exclusive role of unimer exchange[2] is not evident.

Some of the experimental results [5,6,8,11,13,14] turn out to be inexplicable in the framework of a model that considers only unimer exchange. The idea that micelle fusion/fission might take place in block copolymer solutions was suggested[6,22] and confirmed by computer simulations.[9,10]

The objective of the present paper is to analyze the micellization of block copolymers from a solution of unimers by applying a scaling approach and Kramers' theory for calculating the association/dissociation rate constants for both unimer insertion/expulsion and micelle fusion/fission. The analysis goes beyond the consideration of small deviations from the equilibrium state. On the basis of the kinetic equations, the scenario of micelle evolution will be elaborated, and we will compare the results obtained with experimental data. The main qualitative ideas of this model have been already applied for the interpretation of the experimental results presented by Esselink et al.[15,16]

The present paper is organized in the following manner. In the next section, the equilibrium free energy analysis will be presented to illustrate qualitatively the most efficient ways to reach the equilibrium state. In the third section, the activation energy for different micellization processes is considered in the framework of Kramers' theory. In the subsequent section, the association/dissociation rate constants for different mechanisms of micellization are calculated. In the fifth section, the scenario of micelle evolution is elaborated on the basis of kinetic equations. The sixth section is devoted to the discussion of our analytical results in comparison with available experimental data and the results of computer simulations.

Free Energy Analysis

Model System. We will analyze the kinetics of micellar evolution toward equilibrium starting from a unimer solution with concentration exceeding the critical micellar concentration (cmc). Uncharged diblock copolymers capable of micelle formation in a selective solvent (good solvent for B-block and poor solvent for A-block) are considered. The length of A block, N_A, is supposed to be smaller than that for B-block, N_B, ($N_A \leq N_B$). The incompatibility between A-block and solvent (or the other block) leading to micellar formation is characterized by the surface tension coefficient γ, which is assumed to be large, so the standard model of a hairy micelle with narrow interface can be applied in the strong segregation limit.[23,24] The present consideration concerns mainly semidilute solutions rather than concentrated solutions or melts where relaxation processes are rather slow or completely frozen.

We will start with a brief overview of the free energy that describes the equilibrium properties of micellar solution.

Free Energy of Micelle Solution. The free energy of the micellar solution containing identical micelles with aggregation number Q together with free unimers in amount corresponding to the cmc can be written in the following form (cf. Leiber et al[25]):

$$F = N_Q[\ln N_Q + F] + (N - QN_Q)[\ln(N - QN_Q) + F_{\text{un}}] + F_s \tag{5}$$

where F and F_{un} are the free energy per micelle and per unimer, respectively, N_Q is the number density of micelles (i.e., number of micelles per unit volume), and N is the initial polymer number density. The first and the third terms describe the translational free energy for micelles and free unimers, respectively, and F_s is the contribution to the free energy from the solvent.

The free energy of a micelle with an aggregation number Q and the surface tension coefficient γ (ac-

counting for both volume interactions between blocks and between A-block and solvent) can be written in the following form (in units of kT)[23,24]:

$$F = F_{sur} + F_{corona} + F_{core} = C_1 Q^{2/3}(N_A v)^{2/3}\gamma/kT + C_2 Q^{3/2} + C_3 Q^{5/3} N_A^{-1/3} \quad (6)$$

where v is the average volume per monomer unit (which we assume to be the same for both types of monomers) and C_i are coefficients (whose exact values are normally not important in scaling considerations).

The first term in eq 6 corresponds to the surface free energy of a polymer micelle; the second and third terms describe the block extension in the corona and core regions, respectively. For polymer melts, the two latter terms are of the same order, but for polymer solutions, the B-block extension in the corona region is of more importance in defining micelle properties, so that the last term in eq 6 is normally negligible unless the micellar size is very large; i.e., until $Q \le (C_2/C_3)^{3/2} N_A^2$. Thus, in the following, we will neglect the A-block extension as a less important factor in comparison to that for the B-block. (Note, however, that accounting for the A-block extension does not change the main results).

The free energy of a unimer consists mainly of the surface free energy characterizing both A−B block interactions and A-block−solvent interactions:

$$F_{un} \simeq (N_A v)^{2/3}\gamma/kT \quad (7)$$

The minimization of the free energy of the micellar solution F (eq 5) with respect to Q leads to the following well-known scaling law for the aggregation number of the equilibrium micelle:[23,24]

$$Q_{eq} \simeq \left(\frac{2C_1}{3C_2}\right)^{6/5} (N_A v)^{4/5} \left(\frac{\gamma}{kT}\right)^{6/5} \quad (8)$$

The radius of the core and corona region can be expressed in terms of the aggregation number and A-block length as

$$R_{core} \simeq (QN_A v)^{1/3} \qquad R_{corona} \simeq N_B^{\nu} Q^{(1-\nu)/2} v^{1/3} \quad (9)$$

where ν is the Flory exponent for excluded volume ($\nu = {}^3/_5$ for a flexible chain in a good solvent).

By using eq 8, the free energy per polymer micelle (eq 6) and per unimer (eq 7) can be rewritten in the following form:

$$F(Q)/C_2 \simeq \frac{3}{2} Q_{eq}^{5/6} Q^{2/3} + Q^{3/2} \quad (10)$$

$$F_{un} \simeq \frac{3}{2} Q_{eq}^{5/6} \quad (11)$$

The number density of free unimers in equilibrium with polymer micelles, $N_{un} \equiv (N - QN_Q) = \text{cmc}/(N_A + N_B)$, can also be obtained by the minimization of the free energy (with respect to N_Q)[25]

$$N_{un} \simeq \exp(-F_{un} + F(Q_{eq})/Q_{eq}) \simeq \exp(-Q_{eq}^{5/6} + Q_{eq}^{1/2}) \quad (12)$$

Until now, we neglected the polydispersity in the micellar size distribution, which can be characterized by the standard deviation σ, assuming a Gaussian size distribution:[25]

$$\sigma^2 \simeq \left(N_Q \frac{\partial^2 F}{\partial Q^2}\right)^{-1} \sim Q^{1/2}\left(\frac{Q}{Q_{eq}}\right)^{5/6} \quad (13)$$

Although this estimate for σ^2 is fairly rough, it has the correct qualitative dependence: the higher the average aggregation number Q, the broader the micellar size distribution.[15,16]

Free Energy Variation under Micellar Association (Dissociation). To analyze when micellar association or dissociation is favorable, the free energy variation associated with the corresponding process can be investigated. The difference in the combined free energy of two "final" micelles with the aggregation numbers Q_1 and Q_2 and the free energy of the "initial" micelle (with the aggregation number $Q = Q_1 + Q_2$),

$$\Delta F = F(Q_1) + F(Q_2) - F(Q) \quad (14)$$

determines when micelle fission is favorable, i.e., leads to a decrease in the total free energy.[2] ($Q_1 = 1$ or $Q_2 = 1$ corresponds to the unimer expulsion.)

When the increase in the surface free energy upon fission exceeds the decrease in the free energy of B-block extension, $\Delta F > 0$, micellar (or unimer) association is favorable, otherwise ($\Delta F < 0$), micellar fission (unimer expulsion) is preferable.

The free energy variation (in terms of C_2) can be rewritten using eq 10 in the following form (cf. Halperin and Alexander[2]):

$$\Delta F = \frac{3}{2} Q_{eq}^{5/6} Q^{2/3}[X^{2/3} + (1-X)^{2/3} - 1] + Q^{3/2}[X^{3/2} + (1-X)^{3/2} - 1] \quad (15)$$

where $X \equiv Q_1/Q$. ΔF can be considered as a function of X (with a variable parameter Q). The function is symmetric with respect to replacement of X by $1 - X$. An extremum of the function corresponds to $X = {}^1/_2$, which is a maximum for $Q \le Q^* \simeq 0.75 Q_{eq}$ and a minimum for $Q > Q^*$. For $X = {}^1/_2$, the free energy variation ΔF

$$\Delta F|_{X=1/2} = \frac{3}{2} Q_{eq}^{5/6} Q^{2/3}[2^{1/3} - 1] + Q^{3/2}[2^{-1/2} - 1] \quad (16)$$

changes sign from positive to negative at $Q \simeq 2Q^* \simeq 1.5 Q_{eq}$. Thus, for $Q < 2Q^*$, fusion of two equal micelles leads to a decrease in the total free energy, whereas for $Q > 2Q^*$, a micellar fission into two equal micelles becomes favorable.

For $Q > Q^*$, function $\Delta F(X)$ has, in addition to minimum at $X = {}^1/_2$, two (symmetric) maxima at X_{max}. In the limit $Q \gg Q_{eq}$, (where $X_{max} \ll 1$), X_{max} decreases with increasing Q: $X_{max} \simeq (Q_{eq}/Q)^{5/2}$. The absolute value of the free energy variation ΔF at $X = X_{max}$ also decreases as Q increases: $\Delta F|_{X=X_{max}} \sim Q_{eq}^{5/2}/Q$.

The plot of the function $\Delta F(X)$ is shown in Figure 3 for different values of micelle aggregation number Q. For micelles with small aggregation numbers ($Q < Q^*$), ΔF is positive in the whole range of X values (Figure 3a), indicating that coupling of any micelles (or unimer association) is favorable. The most "efficient way" for micellar growth is the fusion of equal micelles, because the free energy gain (through the decrease in the surface free energy) is maximal in this case.

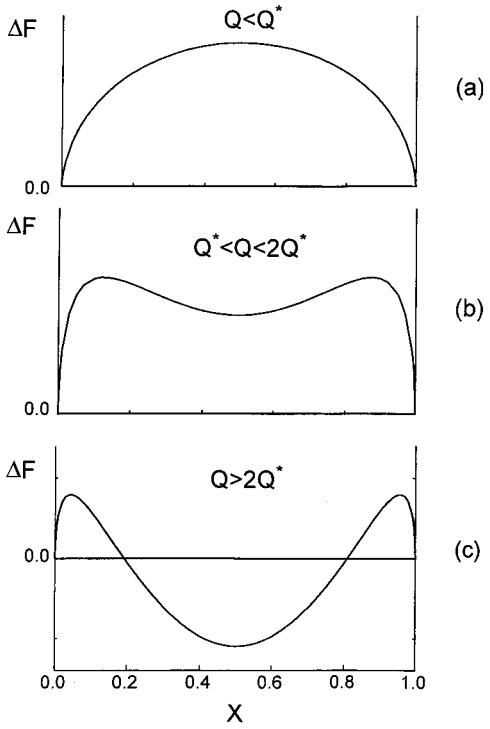

Figure 3. Qualitative plot of the free energy variation for micellar fission of small ($Q \ll Q^*$) (a), intermediate ($Q^* \leq Q \leq 2Q^*$) (b), and large ($Q \gg 2Q^*$) micelles. X is the normalized (in units of Q) aggregation number for one of the emitted micelles.

For $Q^* \leq Q \leq 2Q^*$ (Figure 3b), ΔF is also positive for the whole range of X values, implying that micellar fusion is still favorable for all micelles of smaller size. But now, the maximal gain of the free energy is achieved at $X \neq {}^1/_2$, which corresponds to the fusion of unequal micelles. The reason is that for large micelles there is a considerable increase of block extension that decreases the relative free energy gain.

For $Q > 2Q^*$ (Figure 3c), there are regions of both positive and negative values of ΔF. Indeed, on one hand, fusion with small micelles (unimers) is still favorable because it decreases the total free energy. On the other hand, the most efficient way to decrease the total free energy is fission into two equal micelles with the aggregation numbers close to the equilibrium value because it leads to the considerable decrease in B-block extension. Any fission with formation of small micelle or unimer is unfavorable because the increase in the surface free energy is larger than the decrease in B-block extension. For the same reason, micellar dissociation into unimers is even more unfavorable because this results in a considerable increase in the surface free energy:

$$\Delta F_{\text{uni}}^{\text{dis}} = QF(1) - F(Q) \simeq Q_{\text{eq}}^{5/6}(Q - Q^{2/3}) - Q^{3/2} \quad (17)$$

$\Delta F_{\text{uni}}^{\text{dis}} > 0$ for micelles with an aggregation number less than $Q_{\text{eq}}^{5/3}$. Thus, the dissociation into unimers seems to be particularly unfavorable unless the initial micelle is huge, $Q > Q_{\text{eq}}^{5/3}$.

Thus, the free energy analysis shows that the maximal free energy gain (and hence the most efficient way to reach the equilibrium state) can be attained by (i) fusion of equally sized micelles with aggregation numbers less than $Q^*/2$, (ii) unequal micelles fusion when the size for one of the micelles is larger than $Q^*/2$, and

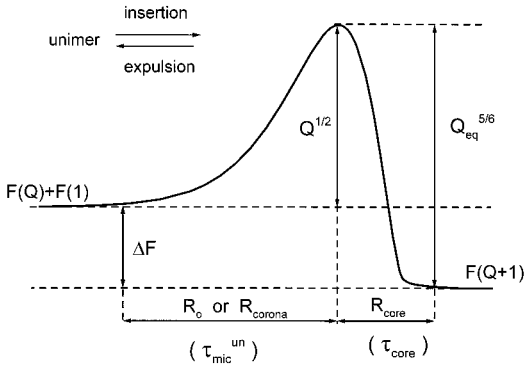

Figure 4. Schematic picture of the potential barrier for unimer insertion/expulsion considered in the framework of Kramers' rate theory.

(iii) fission into equivalent micelles when the aggregation number of the initial micelle is larger than $2Q^* \simeq 1.5Q_{\text{eq}}$.

Energetic Barriers

To estimate the association/dissociation rates, it is appropriate to employ Kramers' theory[26] for systems with high viscosities. To this end, the knowledge of the potential barriers, or more precisely activation energy, for each process is required. The activation energy U appears in the expression for the Arrhenius factor $\exp(-U/kT)$, which is connected with the reaction rate (velocity).[26] The activation energy U can be defined as the highest energetic penalty that has to be paid by a polymer system for the transition from one state to another along the lowest energy pathway. In the next sections, we will consider the activation energies for different processes.

Unimer Insertion/Expulsion. The activation energy for unimer insertion $U_{\text{un}}^{\text{ins}}$ can be defined from the following considerations. For a unimer to enter the micellar core, it has to pass through the corona region. Taking into account that the polymer concentration in the corona region (especially near the micellar core) is higher than average, the penetration into this region is energetically unfavorable and is the main contribution to the potential barrier for unimer insertion. The value of the activation energy $U_{\text{un}}^{\text{ins}}$ is on the order of the free energy of B-block extension in the corona of the micelle:

$$U_{\text{un}}^{\text{ins}} \simeq Q^{1/2} \quad (18)$$

Indeed, as a unimer approaches the micelle core, the conformation of B-block of the unimer changes from coil-like in intermicellar space (free unimer) into extended chain of blobs[27] in the corona region (associated chain). (In the case of unimer coupling, the conformation of B-blocks is not required to change, and hence, there is no potential barrier for the process.) As soon as an A-block of unimer merges with the micelle core, the total of the free energies for unimer and micelle decreases due to the decrease in the surface free energy (Figure 4).

The reverse process of unimer expulsion naturally goes through the same stages as unimer insertion, but in the reverse order. First, the A-block of the unimer has to be released from the core region. As soon as it assumes a globule-like conformation separated from the donor-micelle core, the total free energy increases to a value on the order of the surface free energy of a unimer,

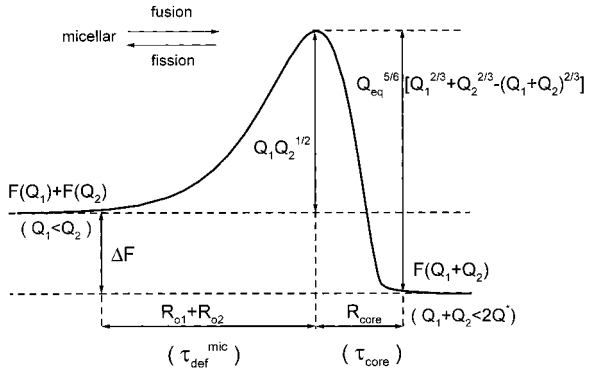

Figure 5. Schematic picture of the potential barrier for micellar fusion/fission considered in the framework of Kramers' rate theory.

which is the activation energy for unimer expulsion:

$$U_{un}^{ex} \simeq Q_{eq}^{5/6} \simeq (N_A v)^{2/3}\gamma/kT \qquad (19)$$

As a unimer proceeds through the corona region (to become free unimer), the extension of B-block decreases and hence the total free energy decreases. The total free energy change for unimer expulsion (which is equal to the difference in activation energies for unimer expulsion and unimer insertion) is ΔF (eq 15 with $Q_1 = 1$).

$$U_{un}^{ex} - U_{un}^{ins} = \Delta F \simeq Q_{eq}^{5/6} - Q^{1/2} \qquad (20)$$

Micellar Fusion/Fission. The energetic barrier for micellar fusion has the same origin as for that for the unimer insertion: for two micelles to merge, one of the micelles (with aggregation number Q_1) has to penetrate the dense corona region of the other micelle (with aggregation number $Q_2 \geq Q_1$). The corresponding activation energy U_{fus}, is on the order of the elastic free energy for Q_1 chains associated into a larger micelle[2,28]

$$U_{fus} \simeq Q_1 Q_2^{1/2} \qquad (21)$$

The conformation of each B-block of the smaller micelle (as soon as it merges with the larger one) becomes more extended (with the free energy loss per chain of $\sim Q_2^{1/2}$), which leads to the total energy loss of $\sim Q_1 Q_2^{1/2}$. Similar to unimer insertion, merging of micellar cores gives significant energetic gain through decrease of surface free energy (Figure 5). The fusion of very small micelles such as dimers or trimers occurs without overcoming any potential barriers because polymer concentration in micelle coronas is close to the average for the solution. In general, the estimation of the activation energy for micelle fusion (eq 21) is correct for the micelles with relatively large aggregation numbers, for which the model of a hairy micelle with well-defined core and corona region is applicable.

Micellar fission starts with the separation of micellar cores, and as soon as this process is accomplished, i.e., when two new micellar cores appears, the total surface free energy increases. The free energy increase corresponds to the activation energy U_{fiss}

$$U_{fiss} \simeq Q_{eq}^{5/6}[Q_1^{2/3} + Q_2^{2/3} - (Q_1 + Q_2)^{2/3}] \qquad (22)$$

The subsequent corona separation decreases the total free energy through entropy gain for B-blocks (which can assume a less extended conformation in the new corona regions). The total free energy change for micellar fission (or in other words the difference between activation energies for micellar fission and fusion) is equal (to an accuracy of numerical coefficients) to ΔF (eq 15.) We note that ΔF can also be negative if the initial micelle is considerably larger than the equilibrium one, i.e., if $Q > 2Q^*$.

Micellar Association from Unimers/Dissociation into Unimers. In principle, it is possible to imagine that a polymer micelle can be formed by the association of Q free unimers all at once (although the probability of such an event is vanishingly small). The activation energy for this process is on the order of the total elastic energy for B-blocks forming the micelle, i.e.,

$$U_{ass} \simeq Q^{3/2} \qquad (23)$$

The simultaneous dissociation of a micelle into Q unimers is also a very rare process, with an activation energy on the order of the Q unimer surface free energies

$$U_{dis} \simeq Q_{eq}^{5/6}[Q - Q^{2/3}] \qquad (24)$$

The difference in dissociation and association activation energies gives, as usual, the total free energy variation ΔF_{uni}^{dis}(eq 17).

Association/Dissociation Rate Constants

To calculate the association/dissociation rate constants for different mechanisms of micellar evolution, besides the activation energy we need to know the characteristic time τ to reach the *activated state*. Then, the rate constant (velocity) of the process can be estimated in the framework of Kramers' theory[26] (large viscosity limit) as

$$r \simeq \frac{\exp(-U)}{\tau} \qquad (25)$$

The *activated state* can be defined as an intermediate state for which formation of the final state or return to the initial state are equally possible. The characteristic times associated with different mechanisms of micelle evolution are discussed in detail in the Appendix. Below, we will use the expressions for activation energies and characteristic times obtained to estimate association/dissociation rate constants for different mechanisms of association.

Unimer Exchange. *Free-Unimers Association*. Micellar evolution from unimer solution ($c >$ cmc) naturally starts from free unimer association. There is no potential barrier for this process, because a polymer chain is not required to enter the regions with a concentration higher than the average concentration. Hence, the association rate constant α_{un}^0 is defined by the inverse time to reach the *activated state*, that is, the diffusion time for unimers to reach each other

$$\alpha_{un}^{0} \simeq \frac{1}{\tau_{dif}^{un}}$$

$$\tau_{dif}^{un} \simeq \frac{\eta_s \nu}{kT} \frac{(N_B + N_A)^{2/3} N_B^{3/5}}{(c\nu)^{2/3}} \qquad \text{for } c < c^*$$

$$\tau_{dif}^{un} \simeq \frac{\eta_s \nu}{kT} N_B^{9/5} \left(\frac{c}{c^*}\right)^{3/2} \qquad \text{for } c \geq c^* \tag{26}$$

As discussed in the Appendix, the unimer diffusion time depends on the average polymer concentration, c, chain length, and viscosity of the solvent, η_s.

Unimer Insertion. Unimer insertion into a micelle requires overcoming the potential barrier (eq 18), because in this case the unimer has to travel into the region with the polymer concentration higher than average. There are two characteristic times associated with unimer insertion: τ_{mic}^{un} and τ_{core}. τ_{mic}^{un} is the time for the unimer to penetrate the micelle corona (eqs A4,A5),

$$\tau_{mic}^{un} \simeq \frac{\eta_s \nu}{kT} Q N_B^{9/5} \frac{(1 - X^*)^2 (1 - X^{*5/3})}{(1 - X^{*3})^{3/2}}$$

$$\text{for } Q < (c\nu)^{5/2} N_B^2;\ X^* \equiv \frac{R_{core}}{R_0}$$

$$\tau_{mic}^{un} \simeq \frac{\eta_s \nu}{kT} Q N_B^{9/5} \frac{(1 - X)^2}{(1 - X^3)^{3/2}}$$

$$\text{for } Q > (c\nu)^{5/2} N_B^2;\ X \equiv \frac{R_{core}}{R_{corona}} \tag{27}$$

whereas τ_{core} is the characteristic time for an A-block of unimer to enter a micelle core and to assume a stretched conformation (eq A6):

$$\tau_{core} = N_A^{7/3} Q^{4/3} \frac{\zeta}{kT} \frac{\nu^{4/3}}{a_{pr}^2} \tag{28}$$

The details of calculation of τ_{mic}^{un} and τ_{core} are discussed in the Appendix. Either τ_{mic}^{un} or τ_{core} can be taken as the time to reach the *activated state*, depending on which value is larger. A more precise definition of the *activated state* for unimer insertion would be a superfluous complication as the difference in numerical coefficients can hardly be distinguished in the framework of a scaling approach. Hence, for the unimer insertion rate constant we have

$$\alpha_{un} \simeq \frac{\exp(-U_{un}^{ins})}{\tau_{un}} \sim \frac{\exp(-Q^{1/2})}{\tau_{un}}$$

$$\tau_{un} = \tau_{mic}^{un} \qquad \text{if } Q < \left(\frac{\eta_s a_{pr}^2}{\zeta \nu^{1/3}}\right)^3 \frac{N_B^{27/5}}{N_A^7}$$

$$\tau_{un} = \tau_{core} \qquad \text{if } Q > \left(\frac{\eta_s a_{pr}^2}{\zeta \nu^{1/3}}\right)^3 \frac{N_B^{27/5}}{N_A^7} \tag{29}$$

The unimer insertion rate constant naturally decreases for longer polymer chains and for larger micelles.

Unimer Release. To become a free unimer, a polymer chain aggregated into a micelle has to pass through the same stages as those for unimer insertion, but in the reverse order and with a different potential barrier to overcome (eq 19). As discussed above, the potential barrier originates from the increase in the surface free energy when the unimer's A-block separates from the core of the micelle donor. The characteristic time to reach *activated state* should be same as that for unimer insertion, τ_{un} (eq 29), according to the "definition" of the *activated state*. Thus, the unimer expulsion rate constant is

$$\beta_{un} \simeq \frac{(\exp - U_{un}^{ex})}{\tau_{un}} = \frac{(-Q_{eq}^{5/6})}{\tau_{un}} \sim \frac{\exp[-(N_A \nu)^{2/3} \gamma / kT]}{\tau_{un}} \tag{30}$$

The larger the equilibrium micelle aggregation number Q_{eq} (i.e., larger surface tension coefficient γ or A-block length), the larger is the energetic barrier to be overcome for unimer release, and hence, the smaller is β_{un}. The expulsion of unimer from larger micelles also proceeds more slowly. The unimer insertion rate constant is connected with that for unimer expulsion via the following relation:

$$\frac{\alpha_{un}}{\beta_{un}} = \exp(\Delta F) \tag{31}$$

where ΔF is the free energy gain upon unimer insertion (eq 15 with $Q_1 = 1$). In fact, β_{un} can be considered as the expulsion rate parameter k^- for the Aniansson–Wall unimer exchange model[17–19] (eq 2), which, however, is valid only for the final stage of micellar evolution where a balance between unimer insertion and unimer expulsion exists.

Micelle Association from Unimers/Dissociation into Unimers. The rate constant for the simultaneous association of Q unimers can be estimated as

$$\alpha_{ass} \simeq \frac{\exp(-U_{ass})}{\tau_{un}} \sim \frac{\exp(-Q^{3/2})}{\tau_{un}} \tag{32}$$

On the face of it, the association of Q unimers all at once seems to proceed without a unimer entering a dense region such as the micelle corona. Nevertheless, τ_{un} is a good estimate for the time to reach the *activated state*, because the presence of Q polymer chains in a small volume inevitably means a higher-than-average polymer concentration, and hence, chains do travel through the region with high polymer concentrations comparable to c_{corona} (the characteristic time is about τ_{mic}^{un}). Then, A-blocks have to form a micelle core with a characteristic time on the order of τ_{core}. The rate constant for simultaneous micellar dissociation into Q unimers is

$$\beta_{dis} \simeq \frac{\exp(-U_{dis})}{\tau_{un}} \sim \frac{\exp(-Q_{eq}^{5/6}[\,Q - Q^{2/3}])}{\tau_{un}} \tag{33}$$

The association and dissociation rate constants are connected via

$$\frac{\alpha_{ass}}{\beta_{dis}} = \exp(\Delta F_{uni}^{dis}) \tag{34}$$

where ΔF_{uni}^{dis} is free energy gain that accompanies the association of Q unimers (eq 17).

Micelle Fusion/Fission. Fusion of very small micelles (dimers and trimers) is similar to free-unimer association and occurs without overcoming any potential barrier. The association rate constant is defined by the corresponding inverse diffusion time for micelles to reach each other

$$\alpha^0_{fus} \simeq \frac{1}{\tau^0_{dif}}$$

$$\tau^0_{dif} \simeq \frac{\eta_s \nu}{kT} \frac{Q^{13/15}(N_B + N_A)^{2/3} N_B^{3/5}}{(c - c_{cmc})^{2/3} \nu^{2/3}}$$

$$\text{for } c < c^*;\ Q \ll Q_{eq}$$

$$\tau^0_{dif} \simeq \frac{\eta_s \nu}{kT} N_B^{9/5} Q^{3/5} (c/c^*)^{3/2}$$

$$\text{for } c \geq c^*;\ Q \ll Q_{eq} \qquad (35)$$

τ^0_{dif} can be obtained in a similar way as the unimer diffusion time (eqs A1 and A2) by taking into account that the average distance between micelles is on the order of $[Q(N_B + N_A)/(c - c_{cmc})]^{1/3}$ for $c < c^*$, and it is about the average micelle size $R_{corona} \simeq N_B^{3/5} Q^{1/5} \nu^{1/3}$ for $c \geq c^*$. τ^0_{dif} is only slightly larger τ^{un}_{dif}.

For micelles with a large aggregation number, fusion requires overcoming the potential barrier (eq 21). There are three characteristic times associated with the fusion process. τ^{mic}_{dif} is the time for micelle diffusion in the region with the average polymer concentration (eq A8). τ^{mic}_{def} is the time for "deformation" of micelle coronas, i.e., the time for cores of neighboring micelles to come into contact (eqs A9−A11). τ_{core} is the characteristic time for micelle cores to merge. The characteristic times mentioned above are calculated in the Appendix. τ^{mic}_{def} is the largest time among the three (unless we deal with very dilute solution where τ^{mic}_{dif} can be on the same order as τ^{mic}_{def}). Hence, τ^{mic}_{def} ($+\tau^{mic}_{dif}$ for $Q < (c\nu)^{5/2} N_B^2$) gives the appropriate estimate for the time to reach the *activated state*. As for unimer exchange, a more precise definition of the *activated state* is not required.

The association rate constant for the fusion of micelles with aggregation number Q_1 and Q_2 ($\geq Q_1$) is

$$\alpha_{fus} \simeq \frac{\exp(-U_{fus})}{\tau^{mic}_{def}} \simeq \frac{\exp(-Q_1 Q_2^{1/2})}{\tau^{mic}_{def}} \qquad (36)$$

$$\tau^{mic}_{def} \simeq \frac{\eta_s \nu}{kT} N_B^{17/5} Q_2^{9/5} (c\nu)^2 \qquad \text{for } Q < (c\nu)^{5/2} N_B^2$$

$$\tau^{mic}_{def} \simeq \frac{\eta_s \nu}{kT} N_B^{9/5} Q_2^{13/5} \qquad \text{for } Q > (c\nu)^{5/2} N_B^2 \qquad (37)$$

For fusion of micelles with relatively small aggregation numbers, $\tau^{mic}_{def} \simeq (\eta_s \nu/kT)\, N_B^{17/5} Q_1^{4/5} Q_2 (c\nu)^2$ (eq A10). The potential barrier for the merging of micelles can be somewhat smaller in this case, as we discussed in the previous section.

α_{fus} decreases as the micelle aggregation number, polymer concentration, or solvent viscosity increases. For the case of $Q_1 \ll Q_2$, the process of micelle fusion is similar to that of unimer insertion in the sense that the smaller micelle has to diffuse through the corona of the larger micelle, rather than simultaneous "deformation" of micelle coronas occurring. The association rate constant for the fusion of micelles that strongly differ in size $Q_1 \ll Q_2$ is

$$\alpha_{fus} \simeq \frac{\exp(-Q_1 Q_2^{1/2})}{\tau_{dif}} \qquad \text{with } \tau_{dif} \simeq \frac{\eta_s \nu}{kT} N_B^{9/5} Q_1^{4/5} Q_2^{4/5} \quad \text{for } Q_1 \ll Q_2 \qquad (38)$$

τ_{dif} is calculated in the Appendix (eq A12).

Micellar Fission. Micellar fission naturally proceeds through the same stages as micellar fusion, but in the reverse order. The characteristic time to reach the activated state is the same as that for micelle fusion, τ^{mic}_{def} (or τ_{dif} for the case of very small micelle expulsion). Taking into account that the activation energy for micellar fission is U_{fiss} (eq 22), we get for the micellar dissociation rate constant

$$\beta_{fiss} \simeq \frac{\exp(-U_{fiss})}{\tau^{mic}_{def}} \simeq \frac{\exp(-Q_{eq}^{5/6}[\, Q_1^{2/3} + Q_2^{2/3} - (Q_1 + Q_2)^{2/3}])}{\tau^{mic}_{def}} \qquad (39)$$

As for unimer exchange, the association and dissociation rate constants are connected via the relation

$$\frac{\alpha_{fus}}{\beta_{fiss}} = \exp(\Delta F) \qquad (40)$$

where ΔF is the total free energy gain from micellar fusion (eq 15).

Micellization Kinetics

To analyze the time evolution of the micelle population during equilibration process, starting from free unimer solution, kinetic equations (similar to that using for chemical reactions) can be employed:

$$\frac{dN_Q}{dt} = \sum_{\tilde{Q}<Q} [\alpha(\tilde{Q}, Q - \tilde{Q}) N_{\tilde{Q}} N_{Q-\tilde{Q}} - \beta(\tilde{Q}, Q - \tilde{Q}) N_Q] + \sum_{\tilde{Q}>Q} \beta(Q, \tilde{Q} - Q) N_{\tilde{Q}} - \sum_{\tilde{Q}} \alpha(Q, \tilde{Q}) N_Q N_{\tilde{Q}} + \alpha_{ass}(Q)(N_1)^Q - \beta_{diss}(Q) N_Q \qquad (41)$$

where N_Q is the number density of micelles with aggregation number Q. $\alpha(Q, \tilde{Q})$ and $\beta(Q,\tilde{Q})$ are the association and dissociation rate constants, respectively, for fusion and fission of micelles with aggregation numbers Q and $\tilde{Q}$. If $Q = 1$ or $\tilde{Q} = 1$, these are the corresponding rate constants for unimer exchange. Association/dissociation rate constants calculated in the previous section for different micellization mechanisms are collected in Table 1.

The first term in each line of eq 41 describes the increase in the number density of micelles with aggregation number Q due to the fusion of two smaller micelles (or two unimers or a unimer and a micelle), fission of a larger micelle (or unimer expulsion), or the simultaneous association of Q unimers, respectively. The second terms in these lines define the decrease in the number density as a result of fission of the micelle (or unimer expulsion), merging with another micelle (or unimer insertion), and dissociation into Q unimers all at once, respectively.

Table 1. Association/Dissociation Rate Constants for Different Micellization Mechanisms

process type	rate constant	time to reach activated state
free unimer coupling	$\alpha_{un}^0 \cong 1/\tau_{dif}^{un}$	$\tau_{dif}^{un} \approx (\eta_s v/kT)(N_A + N_B)^{2/3} N_B^{3/5}(1/cv)^{2/3}$ $c < c^*$
		$\tau_{dif}^{un} \approx (\eta_s v/kT) N_B^{9/5}(c/c^*)^{3/2}$ $c > c^*$
unimer insertion	$\alpha_{un} \cong \exp(-Q^{1/2})/\tau_{un}$	$\tau_{un} \approx (\eta_s v/kT) Q N_B^{9/5}[(1 - X^*)^2(1 - X^{*5/3})/(1 - X^{*3})^{3/2}$ $Q < (cv)^{5/2} N_B^2$; $X^* \approx R_{core}/R_0$
unimer expulsion	$\beta_{un} \cong \exp(-Q_{eq}^{5/6})/\tau_{un}$	$\tau_{un} \approx (\eta_s v/kT) Q N_B^{9/5}(1 - X)^2/(1 - X^3)^{3/2}$ $Q > (cv)^{5/2} N_B^2$; $X \approx R_{core}/R_{corona}$
	$Q_{eq}^{5/6} \cong (N_A v)^{2/3}\gamma/kT$	
		$\tau_{un} \approx (\zeta v^{4/3}/kT a_{pr}^2) Q^{4/3} N_A^{7/3}$ $Q > (\eta_s/\zeta)^3\, a_{pr}^6 v^{-1} N_B^{27/5} N_A^{-7}$
small micelle fusion	$\alpha_{fus}^0 \cong {}^1/\tau_{dif}^0$	$\tau_{dif}^0 \approx (\eta_s v/kT) Q^{13/15} N_B^{3/5}[(N_A + N_B)/(c - c_{cmc})v]^{2/3}$ $c < c^*$; $Q \ll Q_{eq}$
		$\tau_{dif}^0 \approx (\eta_s v/kT) Q^{3/5} N_B^{9/5}(c/c^*)^{3/2}$ $c > c^*$; $Q \ll Q_{eq}$
micelle fusion	$\alpha_{fus} \cong \exp(-Q_1 Q_2^{1/2})/\tau_{mic}$ $Q_1 \le Q_2$	$\tau_{mic} \approx (\eta_s v/kT) N_B^{9/5} Q_1^{4/5} Q_2^{4/5}$ $Q_1 \ll Q_2$
		$\tau_{mic} \approx (\eta_s v/kT) N_B^{17/5} Q_1^{4/5} Q_2 (cv)^2(1 - X')$ $Q_1 \le Q_2 \ll Q_{eq}$
micelle fission	$\beta_{fiss} \cong \exp[-Q_{eq}^{5/6}(Q_1^{2/3} + Q_2^{2/3} - Q^{2/3})]/\tau_{mic}$	$\tau_{mic} \approx (\eta_s v/kT) N_B^{17/5} Q_2^{9/5} (cv)^2(1 - X')$ $Q_2 < (cv)^{5/2} N_B^2$; $X' = R_0/R_{corona}$
	$Q = Q_1 + Q_2$; $Q_1 \le Q_2$	
		$\tau_{mic} \approx (\eta_s v/kT) N_B^{9/5} Q_2^{13/5}$ $Q_2 > (cv)^{5/2} N_B^2$
micelle assoc. from unimers	$\alpha_{ass} \cong \exp(-Q^{3/2})/\tau_{un}$	τ_{un} as for unimer insertion/expulsion
micelle dissoc. into unimers	$\beta_{diss} \cong \exp[-Q_{eq}^{5/6}(Q - Q^{2/3})]/\tau_{un}$	τ_{un} as for unimer insertion/expulsion

At equilibrium, when $dN_Q/dt = 0$, there is a balance between association and dissociation process

$$\alpha(\tilde{Q}, Q - \tilde{Q}) N_{\tilde{Q}} N_{Q-\tilde{Q}} = \beta(\tilde{Q}, Q - \tilde{Q}) N_Q \qquad \text{for } \tilde{Q} \sim Q_{eq} \quad (42)$$

where the micelle size distribution N_Q is defined by a Gaussian function with the standard deviation $\sigma \simeq Q_{eq}^{1/4}$. The value of the standard deviation can be obtained either from the analysis of the equilibrium free energy (eq 13) or using eq 42 and eq 40 (or eq 31):

$$\frac{\alpha(\tilde{Q}, Q - \tilde{Q})}{\beta(\tilde{Q}, Q - \tilde{Q})} = \exp(\Delta F) = \frac{N_Q}{N_{\tilde{Q}} N_{Q-\tilde{Q}}} \sim \exp\left[\frac{Q_{eq}^2}{\sigma^2}\right] \quad (43)$$

As it follows from eq 15, $\Delta F \sim Q_{eq}^{3/2}$ hence, we get (from eq 43) $\sigma^2 \sim Q_{eq}^{1/2}$ in agreement with the result obtained from the equilibrium free energy analysis. When all association/dissociation rate constants as well as the initial micelle size distribution are known, the set of kinetic equations can be solved numerically and the micelle size distribution can be defined for each moment of time. This is a subject for detailed consideration at a later time. In the present paper, we are interested mainly in the prediction of the general qualitative features of the process that can be checked experimentally.

Initial Micellization. To analyze the process of initial micellization as well as to reveal the main features of the equilibration process in general, we will solve numerically the set of kinetic equations related to small Q. We will start from a unimer solution ($N_1 = 1$), and we will study the evolution of the population of micelles with aggregation numbers $1 \le Q \le 35$ toward the equilibrium state ($Q_{eq} \sim 30$). The set of kinetic equations used is self-consistent in the sense that the total number of chains is maintained constant ($\sum_Q Q N_Q = 1$). Formation of micelles of larger size has been allowed, but the fraction of micelles with $Q > 35$ remains negligibly small during the time of calculations. The free unimer association constant, $\alpha(1, 1)$, was chosen to be 0.5; the other association/dissociation rate constants were defined to be consistent with the value of $\alpha(1, 1)$ using eqs 29, 30, 36, 39, and A10 (see also Table 1). [It is necessary to note that in general the activation energy for the association/dissociation of small micelles or for unimer insertion into small micelles is considerably smaller than the value that was obtained in Energetic Barriers and that we used for the calculations (to obey the correct ratio between association and dissociation rates). In reality, the initial micellization would proceed more quickly. So, we expect our results to demonstrate the main trend of the evolution process (accounting for smaller activation energies leads to qualitatively similar results), rather than give us the precise quantitative time dependence of the process.]

The results of numerical solutions of the kinetic equations for "unimer exchange only" (i.e., $\alpha_{fus} = 0$ and $\beta_{fiss} = 0$) are shown in Figure 6. The initial micellization naturally starts from unimer coupling. The rate of the process is defined by the initial unimer concentration and the association constant α_{un}^0, which is the inverse diffusion time for unimers $(\tau_{dif}^{un})^{-1}$. Because the unimer diffusion is relatively quick, the number fraction of unimers decreases rapidly, and correspondingly, the fraction of trimers, tetramers, and especially dimers increases. When the reserve of free unimers is exhausted, the association process becomes effectively frozen due to the lack of free unimers. Indeed, the only source of free unimers is the expulsion from micelles, which is strongly disfavored because of the large increase in surface free energy. As a result, the charac-

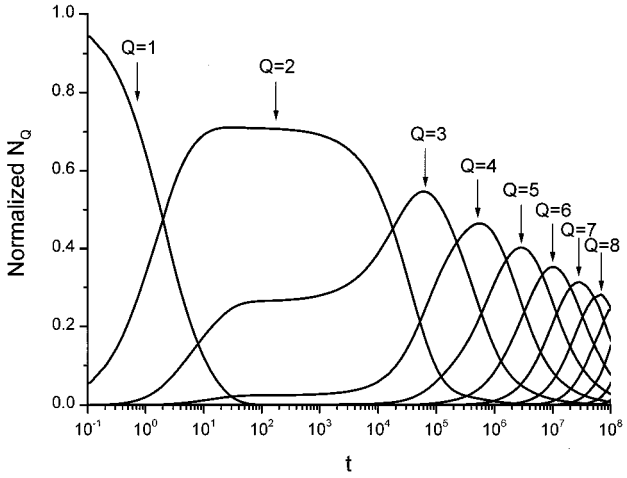

Figure 6. Normalized number density of micelles, $N_Q/\sum_Q N_Q$, as a function of time for the micellization proceeding by unimer exchange only. The results were obtained by numerical solution of kinetic equations for $Q_{eq} = 30$, $N_1(0) = 1$, and $\alpha^0_{un} = 0.5$.

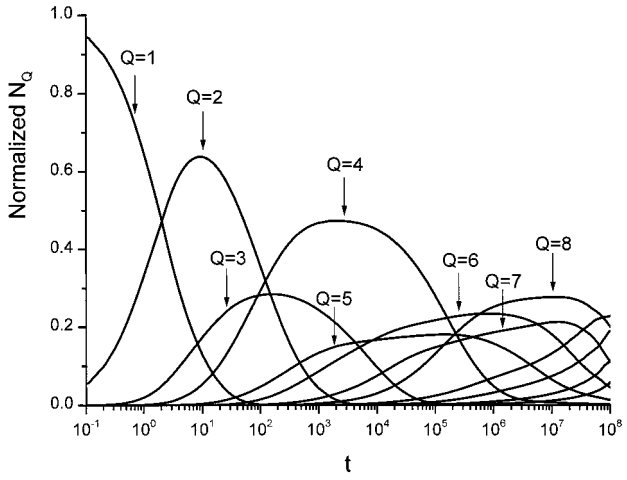

Figure 7. Normalized number density of micelles, $N_Q/\sum_Q N_Q$, vs time for the micellization proceeding by both unimer exchange and micellar fusion/fission. The results were obtained by numerical solution of kinetic equations for $Q_{eq} = 30$, $N_1(0) = 1$, and $\alpha^0_{un} = 0.5$.

teristic time for unimer expulsion is long [$\sim\exp(Q_{eq}^{5/6})$], such that for a significant period of time the polymer system remains in a quasiequilibrium until unimer release becomes kinetically important. Then, the association processes becomes active again, and the fraction of trimers, tetramers, and larger micelles increase at the expense of dimers. The increase in the aggregation number of micelles with the largest number density is gradual: when the number of dimers decreases, timers become the dominant fraction, later tetramers prevail, then pentamers, and so on. Hence, each time the aggregation number of the dominant (in number) micelles increases on a unit until the true equilibrium is reached.

Now, let as consider the solution of the set of kinetic equations accounting for both unimer exchange and micelle fusion/fission, which is presented in Figure 7. The results are remarkably different from those of unimer exchange only (Figure 6). Indeed, first of all, there is no a period of quasiequilibrium, and the association process goes smoothly and proceeds quickly. In contrast to the unimer exchange mechanism, Figure

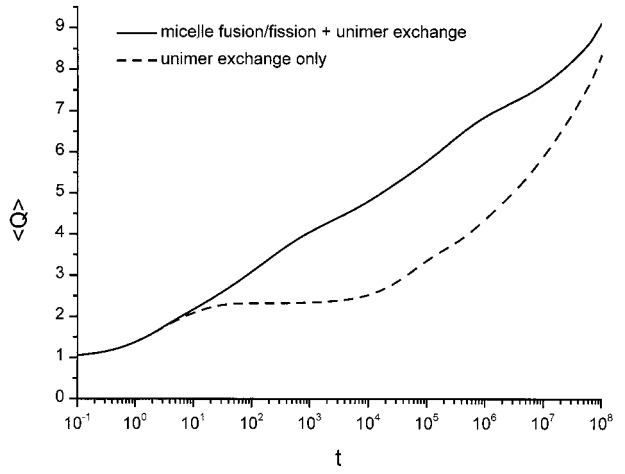

Figure 8. Average aggregation number of micelles as a function of time for "unimer exchange only" (dashed curve) and "micellar fusion/fission + unimer exchange" (solid curve). The results were obtained by numerical solution of kinetic equations for $Q_{eq} = 30$, $N_1(0) = 1$, and $\alpha^0_{un} = 0.5$.

7 shows that dimers are dominant only for a relatively short time, trimers never prevail, and it is the aggregates of four unimers that increase most rapidly in number as dimers decline. Then, tetramers gave way to hexamers as a dominant micelle fraction for a short time, and later, aggregates of eight unimers become paramount. It is interesting to note that neither pentamers nor heptamers prevail. As is seem from Figure 7, the main trend of the process is the association of micelles with the largest number density. Indeed, coupling of dimers gives rise to tetramers, which in their turn can either merge together forming octamers or can fuse with dimers (whose fraction is still considerable) to form hexamers. The latter process has smaller activation energy, and hence, it dominates. Therefore, there are two main tendencies in micelle fusion. (i) The association of averaged micelles is the first tendency. In this case the initial size distribution is single Gaussian-like, and at the end of the characteristic time step, the average aggregation number duplicates ($Q \rightarrow 2Q$). (ii) The association of (growing in number) micelles that will dominate at the next period of time with (decreasing in number) micelles that were dominant at the previous time interval is the second tendency. In this case, the initial size distribution has bimodal character, which is typical for the intermediate state of the abovementioned process of duplication in aggregation number. As a result, the average aggregation number increases to a smaller value ($Q_1, Q_2 \rightarrow Q_1 + Q_2$).

The difference in the intermediate results and the rate of association process proceeding by "unimer exchange only" (Figure 6) and by "micelle fusion/fission + unimer exchange" (Figure 7) is even more clear from Figure 8. As is seen from Figure 8, at the beginning of the equilibration process, the average aggregation number $\bar{Q}$ changes in the same way for both mechanisms of association. When $\bar{Q}$ reaches 2, unimer exchanges turns out to be effectively "frozen" for a period of time, so the average aggregation number remains constant for unimer exchange mechanism. During this time, only the micelle fusion mechanism is active, and it proceeds reasonably quickly: the average aggregation number continuously increases. The inhomogeneity in the rise of the average aggregation number confirms the steplike character of the micelle fusion leading to the duplication

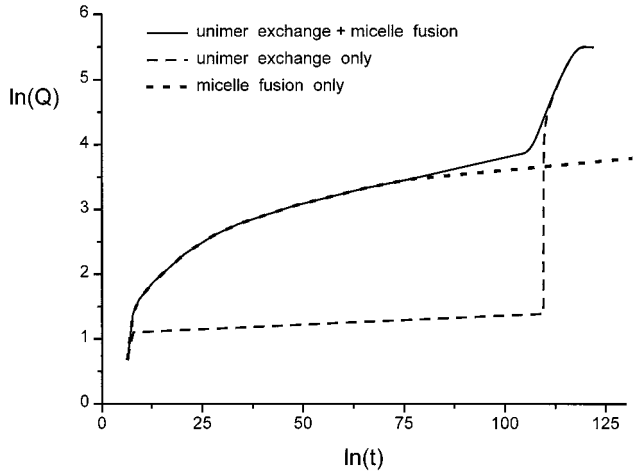

Figure 9. Log−log plot for the number density of micelles vs time for the unimer exchange model (dashed curve, calculated on the basis of eq 45), for the model of averaged micelles fusion (dotted curve, calculated on the basis of eqs 47 and 48) and for the combined association (solid curve), $Q_{eq} = 256$.

of the average aggregation number. When the unimer exchange starts to influence the kinetics, the average aggregation number for unimer exchange mechanisms increases rapidly at a rate exceeding that for the joint mechanism of association, which slows because of the increase in activation energy for both micelle fusion and unimer insertion into micelles with larger average aggregation numbers.

Micellization Scenario. On the basis of the results of numerical calculations considered above, we can identify the general features of the micelle evolution process. Let us consider first the unimer exchange mechanism only. As it was discussed above, after the initial formation of dimers, unimer insertion is limited by the presence of free unimers, which can arise only after their expulsion from a micelle. Because the activation energy for unimer release is large, the unimer exchange begins to work only after considerable time, $\sim\exp(Q_{eq}^{5/6})$. The characteristic step of the process consists of the increase in the average aggregation number on a unit. The kinetic equation for averaged micelle is the following:

$$\frac{dN_{Q+1}}{dt} = \alpha(Q, 1)N_Q N_1 - \beta(Q+1, 1)N_{Q+1} + \beta(Q+2, 1)N_{Q+2} - \alpha(Q+1, 1)N_{Q+1}N_1 \quad (44)$$

The unimer number density N_1 is in fact defined by the cmc: $N_{un} \simeq \exp(-Q_{eq}^{5/6} + Q_{eq}^{1/2})$ (eq 12). Then, the characteristic time per step of unimer association (i.e., to have $Q+1$ become the average aggregation number if in the previous step it was Q) is on the order of

$$\Delta t \sim \tau_{mic}^{un} \exp[Q_{eq}^{5/6} - Q_{eq}^{1/2} + Q^{1/2}] \qquad \overline{Q(t)} = Q + 1 \quad (45)$$

As is seen from eq 45, the time for each step of unimer association depends strongly on Q_{eq}, and it increases with an increase of Q. The total time for unimer association can roughly be estimated as a sum of characteristic times for the successive steps of the evolution. The time dependence of the average aggregation number for the unimer exchange mechanism (for $Q_{eq} = 256$) is presented in Figure 9 (dashed curve). The dependence is qualitatively similar to that obtained by the numerical solution of kinetic equations (Figure 8): a long period of "waiting" for unimer expulsion followed by rapid unimer−micelle association.

If we wish to consider only the micelle fusion mechanism leading to duplication in the average aggregation number, then the characteristic time for the evolution step can be estimated from the kinetic equation for micelles with an aggregation number 2 times larger than the average aggregation number

$$\frac{dN_{2Q}}{dt} = \sum_{\delta=0}^{Q-1}[\alpha(Q-\delta, Q+\delta)N_{Q-\delta}N_{Q+\delta} - \beta(Q-\delta, Q+\delta)N_{2Q}] + \sum_{\tilde{Q}>Q}\beta(Q, \tilde{Q}-Q)N_{\tilde{Q}} - \sum_{\tilde{Q}>1}\alpha(2Q, \tilde{Q})N_{2Q}N_{\tilde{Q}} \simeq \sum_{\delta=0}^{Q-1}\alpha(Q-\delta, Q+\delta)N_{Q-\delta}N_{Q+\delta} \quad (46)$$

The first term in the equation turns out to be the largest one because the potential barrier for micellar fission is rather large. The association of the micelle (with aggregation number $2Q$) with others is possible, but the number fraction of the micelles is much smaller than that for the average micelle (with aggregation number Q). To make an estimation of the characteristic time associated with this process, we have to know the number density distribution N_Q. As a rough approximation, we can consider normalized Gaussian distribution (which is reasonably good in the vicinity of the equilibrium state[15,16,25]) multiplied by the total number density of micelles $N_{mic}(t)$, which is proportional to the total polymer number density N (less N_{un}). The width of the distribution can be estimated as $\sigma \simeq Q^{2/3}Q_{eq}^{-5/12}$ (eq 13). Then, the characteristic time for the evolution step leading to duplication in the average aggregation number is

$$\Delta t \simeq \frac{Q^{2/3}}{N\,Q_{eq}^{5/12}}\left[\sum_{\delta=0}^{Q-1}\alpha(Q-\delta, Q+\delta)\exp\left(-\frac{\delta^2}{\sigma^2}\right)\right]^{-1} \quad (47)$$

For relatively small Q, the quickest time for association step is achieved by association of the averaged micelles (with $\delta = 0$). Thus,

$$\Delta t \sim \frac{Q^{2/3}\tau_{def}^{mic}}{N\,Q_{eq}^{5/12}}\exp(Q^{3/2}) \qquad \overline{Q(t)} = 2Q \quad (48)$$

However, at later times, the contribution due to fusion of micelles differing in size ($\delta \neq 0$) begins to dominate. The remarkable feature of the time dependences (eqs 47 and 48) is that for micelles with $Q > (cv)^{5/2}N_B^2$ (for which τ_{def}^{mic} is concentration-independent) the increase in polymer concentration decreases the characteristic time. This effect is most important in low-concentration solutions.

As is seen from eqs 47 and 48 and Figure 7, each successive step of the evolution takes a significantly longer time. The logarithmic time dependence of the average micelle aggregation number (obtained by summation of the characteristic times for the successive steps) is shown in Figure 9 (dotted curve) for $Q_{eq} = 256$. As is seen there, the increase in average aggregation

number considerably slows with time due to an increase in activation energy for micelle fusion.

Accounting for both unimer exchange and micelle fusion leading to the duplication in the average aggregation number gives us the result presented as a solid curve in Figure 9. From the beginning until the time the unimer exchange becomes active, i.e., until the average aggregation number is smaller than $Q_{eq}^{5/9}$, the micellization proceeds via micelle fusion leading to duplication in average aggregation number. Then, both of the mechanisms act in parallel, and at the final stage, the unimer exchange dominates. It is necessary to note that the result presented in Figure 9 is oversimplified due to inaccuracy in estimation of evolution time steps and because it neglects the other mechanism of micelle fusion characterized by a bimodal size distribution and leading to the increase of the average aggregation number as $Q_1, Q_2 \rightarrow Q_1 + Q_2$. Both of the mechanisms of micelle fusion act in parallel, and hence, to predict the results analytically is a somewhat complicated task. Accounting for unequal micelles fusion would most probably make the dependence presented in Figure 9 more smooth because it increases the contribution of the micelle fusion mechanism at later stages of equilibration.

Hence, it seems to be evident that micelle fusion is the dominant (and in fact the only) mechanism that acts until unimer expulsion becomes active. Later, both micelle fusion of averaged and especially unequal micelles together with unimer exchange contribute to the evolution process. To distinguish the relative contribution of the different mechanisms of micellization and to estimate the "transition point" at which unimer association begins to dominate micelle fusion is fairly difficult to do analytically. All of the processes act in parallel, and the results can strongly be influenced by the fluctuations in size distribution. Our main point is that both mechanisms of micellization are important and neglecting either of them would lead to erroneous conclusions.

Qualitative Comparison to Experiment

The scenario of micellar evolution considered above will now be discussed in context of real polymer systems that have been investigated experimentally. However, it is important to take into account that direct comparison between the analytical results and the experimental data is not always possible because most of the block copolymers studied experimentally are charged and the presence of the electrostatic interactions might have an additional influence on the micellization kinetics.

One of the methods applied to study the kinetics of micellar equilibration is temperature-jump.[8,13,14] A recent paper[8] contains a wealth of information, obtained by using both types of T -jump experiments: with decrease in temperature (increase Q_{eq}) and that in the opposite direction. T-quenching experiments resulting in an increase of Q_{eq} (decrease in the cmc) reveal that for low polymer concentration and with a large temperature change the average micellar molecular weight increases somewhat faster than the average radius of gyration, which first decreases and only later increases at slow rate. Such behavior implies formation of new micelles. For higher polymer concentrations and smaller temperature jumps, both the average micelle molecular weight and the radius of gyration gradually increase. The increase in the average micelle aggregation number (as well as in the width of size distribution $\sigma \simeq Q_{eq}^{1/2}$) can be ensured by unimer coupling (followed by fusion of small micelles) and unimer insertion into existing micelles with the average aggregation number Q_{eq}^* (by the asterisk we denote the parameters corresponding to the "original" state, i.e., before the temperature jump). Unimer association with the averaged micelles is dominant if

$$c - c_{cmc}^* > c^{**} \equiv c_{cmc} \frac{\tau_{mic}^{un}(Q_{eq}^*)}{\tau_{dif}^{un}} Q_{eq}^{*1/4} \exp(Q_{eq}^{*1/2}) \qquad (49)$$

Thus, for a high polymer concentration, with a significant micellar fraction the fastest route to reach new equilibrium is through the association of unimers with already existing micelles. This conclusion is in agreement with the observed difference between the relaxation time for direct micellization and that for the equilibration after a T -jump.[8] The latter turns out to be much faster, because in this case there is a reserve of free unimers and there is no need to "wait" when a unimer will be expelled from the smaller micelle to associate with the larger micelle for equilibration to proceed.

If $c - c_{cmc}^* < c^{**}$, unimer coupling dominates over the association with micelles. As soon as all unimers exceeding the new cmc are associated, the average aggregation number for new small micelles increases as during direct micellization (Figure 7), i.e., according to the scheme 2→4→6→8.... The formation and evolution of new small micelles leads first to a decrease in the average radius of gyration followed by slow increase, as observed.[8] Of course, unimer exchange is also possible, and moreover, it becomes the fastest process when the average aggregation number for small micelles becomes larger than some critical value Q_{cr}

$$N_{Q_{cr}} \frac{\exp(-Q_{cr}^{3/2})}{\tau_{dif}^{mic}(Q_{cr}, Q_{cr})} \simeq N_1 \frac{\exp(-Q_{cr}^{1/2})}{\tau_{mic}^{un}(Q_{cr})} \qquad (50)$$

Then, further evolution proceeds by fusion and chain exchange of new and "old" micelles (with a possible decrease in the number of micelles due to micelle fusion) until a new equilibrium is reached.

T-jump experiments with a temperature increase lead to a decrease in Q_{eq} (an increase in the cmc). For this case, at the beginning, the average molecular weight and the radius of gyration decrease in parallel,[8] meaning that there is an increase in the number of micelles accompanied by the decrease in the aggregation numbers. The phenomenon cannot be explained by unimer exchange, which does not change the number of micelles, and it has been assigned[8] to micellar dissociation into unimers in accordance with Aniansson−Wall model.[17−19] As we already discussed above, the rate constant of micellar dissociation into unimers $\beta_{diss} \sim \exp(-QQ_{eq}^{5/6})$ is smaller than that for micelle fission $\beta_{fiss} \sim \exp(-Q^{2/3}Q_{eq}^{5/6})$. Hence, we can expect that micelle fission rather than micelle dissociation into unimers is responsible for the increase in the number of micelles. This way also seems to be more natural, because the micelles emerging after fission are closer to final equilibrium state than unimers.

As we discussed above, the most efficient way to decrease the free energy of the system is fission into equal micelles, but the time associated with the process is rather large. Micelle fission with expulsion of a small

micelle is less effective in decreasing of the free energy, but the rate is only somewhat smaller [$\simeq(\beta_{un})^{Q^{2/3}}$] than that for unimer expulsion (β_{un}). To estimate analytically the relative contribution of micelle fission and unimer expulsion is a rather complicated task because they act in parallel and knowledge of micelle size distribution at each moment is required.

During the later stages of the equilibration process, the radius of gyration increases quicker than the micelle molecular weight, this indicates a decrease in the number of micelles with an increase in the aggregation number.[8] This is most probably the result of coupling of small micelles (initially expelled from the larger ones or already existing). The comparison of the direct micellization with reequilibration reveals that at low concentration the reequilibration goes slower.[8] Again, this observation seems to support the micelle fission/fusion mechanism. As we discussed above, the characteristic time step for micelle fusion (in diluted solution) is inversely proportional (eqs 47 and 48) to concentration, $\sim 1/N_Q\alpha_{fus}$ (whereas that for unimers is almost concentration-independent). During direct micellization from unimers, the fusion proceeds via fusion of the micelles having the largest number density, but after a *T*-jump, the concentration of expelled or already existing small micelles is much smaller and hence the longer the evolution time.

Similar behavior of micellar solutions has been observed following a large dilution,[15] leading also to the decrease in the equilibrium aggregation number. It was found that immediately after dissolution the average micellar size rapidly decreases, with a distinguishable increase in the fraction of micelles smaller than those in the new equilibrium and almost 2 times smaller than the initial equilibrium micelles.[15] A quick increase in the fraction of smaller micelles supports the micellar fission mechanism (possibly with subsequent fusion). Further micellar growth and reequilibration proceeds in a manner similar to direct micelle evolution: mainly via unimer exchange and to a lesser extent by micellar fusion.

T-jump experiments in triblock copolymer systems[13,14] reveal that the micelle equilibration after a temperature increase seems to follow a similar scenario as that for diblock copolymers.[8] Despite the natural similarity between di- and triblock copolymers, the latter might have more complicated kinetics. First, consider unimer release: both the characteristic time and the potential barrier for B−A−B unimer release is larger than that for an A−B unimer. Indeed, to relieve an A-block from the core of a large micelle not only A but most likely also one of the B-blocks has to move through the core region. If the A- and B- blocks are incompatible, then the additional potential barrier has to be overcome for the B-block movement through the core. This complication can be less crucial for micelle fission: when a part of the micelle core separates, only some of the separating chains (not necessarily all) have to be disentangled, and the potential barrier is smaller than that for chain separation one by one. Hence, micelle fusion/fission seems likely to be even more important for triblock copolymer kinetics.[14]

It is also worthwhile to compare the predictions of our model with recent data from dynamic Monte Carlo simulations.[10] The semianalytical approach has been applied to determine the relative contribution of the different mechanisms of micellar evolution. The transition-rates matrix (for three types of micelles, namely, small, large, and medium, as well as for free polymer chains) has been obtained on the basis of the data of computer simulations. The calculations have been performed at the dynamic equilibrium in the model polymer system,[10] and hence, the results are related to the final stage of micellization evolution in dilute solutions. It was found[10] that for very dilute solutions (with polymer concentrations slightly above the cmc) unimer exchange is the dominant mechanism, whereas for somewhat higher polymer concentrations (but still in dilute regime), micellar fusion/fission takes over. This result seems to be in agreement with our prediction that the characteristic time for micellar fusion in diluted solutions might decrease as the concentration increases (eqs 47 and 48), and hence, the contribution of micellar fusion to the equilibration process increases. [However, this is correct only for $cv < (\bar{Q})^{2/5}N_B^{-4/5}$; further increases in concentration can have the opposite effect due to the strong concentration dependence of τ_{def}^{mic}.] It was also found in the computer simulations[10] that unimer exchange is faster than micellar fusion/fission at nearly equilibrated state.

The influence of the interaction parameter *e* (which can be compared with the surface free energy for our model γ) and insoluble block length N_A manifests itself in an increase of the characteristic times for both unimer exchange and micelle fusion/fission as *e* and N_A increase.[10] This effect is rather natural as it follows, e.g., from the comparison of rate constants (see Table 1). This phenomenon was also observed during the experiments investigating mixed micelles formation.[4,5,16]

One of the interesting features of the comicellization process in the mixtures of originally small and large micelles (with aggregation numbers Q_1 and $Q_2 > Q_1$) is that it always proceeds via the transport of chains from large to small micelles.[5] On the first sight, it is a surprising result because the rate of unimer expulsion from micelles with smaller equilibrium aggregation numbers is naturally higher than that for unimer expulsion from a large micelle (especially if it is formed by triblock copolymers). However, the unimer insertion rate for entering a small micelle is also much higher than that for entering larger micelles, and a unimer expelled from a small micelle is very likely to enter a small micelle again. Unimers or micelles expelled from the larger micelle will also prefer to associate with small micelles because the corresponding association rates (see Table 1) are higher than those for a "return" to a large micelle. So, the comicellization operates at the expense of larger micelles, as was observed.[5]

During the set of experiments, the influence of the aggregation number of the larger micelle Q_2 on hybridization kinetics was studied.[5] It was found that if Q_2 is reasonably large there are two sedimentation peaks approaching each other with time. In this case, the process of chain (or small micelles) transfer discussed above can "visually" be observed. (The longer the time required for the reequilibration, the larger the contribution of micelle fission to the process.) If Q_2 is larger, the third sedimentation peak appears between the two initial ones and grows at their expense. This effect can hardly be explained in the framework of unimer exchange only, whereas micelle fission is the most probable reason for it. As we discussed above, fission into equal micelles is the most efficient way to decrease the free energy, but it requires considerable time. Fission

with emission of small micelles is quicker, and such a micelle can merge with another small micelle. Both types of fission can lead to formation of the third peak. For a very large Q_2, no hybridization can be observed during the experimental time. In this case, any dissociation rates are probably so small that the kinetic process is effectively frozen. Yet, it is necessary to keep in mind that hybridization is not always thermodynamically preferable for the polymer system.[16] Nevertheless, some of the micelle pairs that do not hybridize after mixing the micelles do form hybrid micelles if the initial solution contains only the corresponding unimers. In this case, the association rates dominate, and evolution proceeds via equal micelle fusion at the beginning, with further "correction" of the micelle composition and size distribution by unimer exchange and unequal micelle fusion.

Conclusion

The kinetics of micellar evolution from unimer solution was studied analytically on the basis of a scaling approach applying Kramers' theory for the calculation of the association/dissociation rate constants (see Table 1). The rates constants obtained can be used for the direct numerical solution of the kinetic equations. By analyzing the kinetic equations, the scenario of micelle evolution was elaborated.

The present model should be considered as the complementary analysis to the traditional Aniansson−Wall and Kahlweit kinetic theories for surfactant micelles, because it deals with nonequilibrium states and we consider block copolymer micelles by taking into account both unimer exchange and micelle fusion/fission (the latter was neglected in the Halperin−Alexander theory). The numerical solution of the kinetic equations for a small micelle population as well as analytical estimations show that the intermediate results and evolution rate for the mechanism of "unimer exchange only" strongly differ from that for joint mechanism of "micelle fusion/fission + unimer exchange". The model of "unimer exchange only" reveals that after free unimer coupling is accomplished, unimer association becomes effectively frozen for a long time due to the high activation energy for unimer release. According to the joint mechanism of association, the evolution proceeds mainly via the fusion of micelles with the largest number density until the average aggregation number becomes larger than $Q_{eq}^{5/9}$ (later, unimer exchange becomes kinetically important because micelle fusion/fission has slowed). One of the mechanisms of micelle fusion is the association leading to the duplication in the average aggregation number ($Q \rightarrow 2Q$). The characteristic times for the evolution step for the micelle fusion (and unimer exchange) is estimated. It was found that micelle fusion is strongly concentration-dependent. The other mechanism of micelle fusion is association of unequal micelles. This process is active when the size distribution has bimodal character. In this case, the aggregation number increases as Q_1, $Q_2 \rightarrow Q_1 + Q_2$. Both mechanisms of micelle fusion together with unimer exchange (which is the quickest process) contribute to the final stage of association.

Micelle fission is a relatively slow process unless a very small micelle is emitted. The influence of micelle fission becomes important during reequilibration of micelles with a decrease in the average aggregation number such as occurs with a heating *T*-jump experiment.

The comparison of the predictions of the present theoretical model with the data of *T*-jump experiments, investigations of comicellization phenomena, and the results of computer simulations shows that in all cases considered there is a good qualitative agreement and the model seems to be rather successful in the explanation of the phenomena observed.

Acknowledgment. I am grateful to Prof. G. ten Brinke, Prof. G. Hadziioannou, Dr. F. Esselink for stimulating discussions. I am indebted to Prof. S. E. Webber for helpful discussions and valuable comments that initiated me to generalize and refine the approach. Financial support by FOM-NWO (Netherlands Organization for Scientific Research) is gratefully acknowledged.

Appendix: Characteristic Times for Unimer Insertion/Expulsion and Micelle Fusion/Fission

Free-Unimers Association. To merge with other unimer(s), a unimer has to diffuse an average distance between unimers in solution. The corresponding distance is on the order of $[(N_B + N_A)/c]^{1/3}$ for solutions with polymer concentration c less than the polymer overlap concentration $c^* = 1/N_B^{3\nu-1}v$. The diffusion coefficient for unimer is $D_o^{un} = kT/\eta_s N_B^{\nu} v^{1/3}$.[29] Hence, the characteristic time for free-unimers association is

$$\tau_{dif}^{un} \simeq \frac{\eta_s v}{kT} \frac{(N_B + N_A)^{2/3} N_B^{3/5}}{(cv)^{2/3}} \qquad \text{for } c < c^* \qquad \text{(A1)}$$

The unimer diffusion time increases with increases in the chain length and viscosity of the solvent and with a decrease in polymer concentration.

When $c \geq c^*$, the average distance for a unimer to diffuse is on the order of a chain size, $N_B^{3/5} v^{1/3}$, and the diffusion coefficient (for $\nu = {}^3/_5$) is[30]

$$D^{un} = kT/\eta_s N_B^{3/5} v^{1/3} (c/c^*)^{3/2} \qquad \text{(A2)}$$

Hence, for $c \geq c^*$, the characteristic time associated with unimer fusion is[29,30]

$$\tau_{dif}^{un} \simeq \frac{\eta_s v}{kT} N_B^{9/5} \left(\frac{c}{c^*}\right)^{3/2} \qquad \text{for } c \geq c^* \qquad \text{(A3)}$$

Unimer Insertion into a Micelle. *Penetration into Micelle Corona.* The initial state for the unimer insertion is a unimer in contact with the corona periphery only. The average distance between unimer and micelle can be larger; however, the potential barrier appears (and the diffusion time considerably increases) only when a unimer enters the region of higher-than-average polymer concentration. For $Q < (cv)^{5/2} N_B^2$ this distance is equal[27] to $R_0 \simeq v^{1/3} Q^{1/2}/(cv)^{3/4}$, whereas for $Q > (cv)^{5/2} N_B^2$, this is the total radius of micelle R_{corona}.

To merge with a micelle with aggregation number $Q > (cv)^{5/2} N_B^2$, a unimer has to pass through the whole corona region, i.e., the distance $R_{corona} - R_{core}$. The average polymer concentration increases as the micelle core is approached, and hence, the diffusion process is gradually slowing. To simplify the analysis, we will assume, however, that the concentration in the corona region is equal to the average concentration $c_{corona} \simeq QN_B/(R_{corona}^3 - R_{core}^3)$. Then, the diffusion coefficient is equal to D^{un} (with replacement of c by c_{corona}), and the diffusion time is

$$\tau_{\text{mic}}^{\text{un}} \simeq \frac{\eta_s v^{1/3}}{kT}(R_{\text{corona}} - R_{\text{core}})^2 N_B^{3/5}(c_{\text{corona}}/c^*)^{3/2} = \frac{\eta_s v}{kT} Q N_B^{9/5} \frac{(1-X)^2}{(1-X^3)^{3/2}} \quad (\text{for } Q > (cv)^{5/2}N_B^2)$$

$$\text{where } X \equiv \frac{R_{\text{core}}}{R_{\text{corona}}} = \frac{N_A^{1/3} Q^{2/15}}{N_B^{3/5}} \quad \text{(A4)}$$

For insertion into the micelle with aggregation number $Q < (cv)^{5/2}N_B^2$, a unimer has to travel the distance $R_0 - R_{\text{core}}$. Again, we will estimate the diffusion time by assuming that the motion occurs in the medium with the average concentration $c_{\text{mic}} \simeq QN_B^*/\Delta V = Q^{2/3}R_0^{-4/3}[1 - (R_{\text{core}}/R_0)^{5/3}]/[1 - (R_{\text{core}}/R_0)^3]$ [where $N_B^* \simeq Q^{-1/3}(R_0^{5/3} - R_{\text{core}}^{5/3})$ is the number of monomer units of B-block inside the sphere of radius R_0]. Correspondingly, the diffusion coefficient is equal to D^{un} (with replacement of c by c_{mic}), and for the diffusion time we get the following:

$$\tau_{\text{mic}}^{\text{un}} \simeq \frac{\eta_s v^{1/3}}{kT}(R_0 - R_{\text{core}})^2 N_B^{3/5}(c_{\text{mic}}/c^*)^{3/2} = \frac{\eta_s v}{kT} Q N_B^{9/5} \frac{(1-X^*)^2(1-X^{*5/3})}{(1-X^{*3})^{3/2}} \quad (\text{for } Q < (cv)^{5/2}N_B^2)$$

$$\text{where } X^* \equiv \frac{R_{\text{core}}}{R_0} = \frac{N_A^{1/3}(cv)^{3/4}}{Q^{1/6}} \quad \text{(A5)}$$

$\tau_{\text{mic}}^{\text{un}}$ increases with an increase in the aggregation number, solvent viscosity, and chain length.

Penetration into Micelle Core. To accomplish merging, an A-block of the unimer has to penetrate the micelle core. The penetration proceeds through the reptation motion of the A-block. Taking into account that the average size of an A-block forming a micelle is on the order of the micellar core size, the length of the primitive path to be passed is $l_{\text{pr}} \simeq R_{\text{core}}^2/a_{\text{pr}}$ (where a_{pr} is the step length of the primitive path). $a_{\text{pr}} \simeq v^{1/3}N_e^{1/2}$, where N_e is the number of monomer units between entanglements. N_e depends mainly on the presence of solvent inside the micelle,[31,32] $N_e \sim c_{\text{core}}^{-1}$ (c_{core} is the polymer concentration inside the core). Because here we consider a strong segregation limit by assuming the absence of solvent in the core region, a_{pr} will be treated as a constant. The diffusion coefficient for this motion is $D_{\text{rep}} \simeq kT/N_A\zeta$, where ζ is the monomer friction coefficient. Hence, the characteristic time for A-block penetration is[29,31,32]

$$\tau_{\text{core}} \simeq \frac{l_{\text{pr}}^2}{D} \simeq N_A^{7/3}Q^{4/3}\frac{\zeta}{kT}\frac{v^{4/3}}{a_{\text{pr}}^2} \quad \text{(A6)}$$

τ_{core} increases with increases in A-block length and the aggregation number Q. [For B−A−B triblock copolymers, the corresponding motion is even more complicated: possibly one of the B-blocks has to pass the same path as a middle A-block. The corresponding time is large: $\tau_{\text{core}} = N_A^{4/3}(N_A + N_B)(\zeta/kT)(v^{4/3}/a_{\text{pr}}^2)$. Another possibility is to wait for a period of time corresponding to "tube" reorganization, $\tau_R \sim \tau_{\text{core}}N_A^2/N_e^2$, which is however larger than τ_{core}.][29,33]

Micelle Fusion/Fission. *Micelle Diffusion for $Q \gg 1$.* The initial state for micellar fusion is two micelles with corona regions in contact. The average distance between micelles can be (much) larger, but because the motion in the dense regions inside the corona is much slower than that in the intermicellar space, this difference in the definition of the initial state is not important. As we discussed above, for micelles with $Q < (cv)^{5/2}N_B^2$ the region where the polymer concentration is higher than average is the area inside the sphere of radius R_0, whereas for $Q > (cv)^{5/2}N_B^2$, this is the whole corona region R_{corona}. Fusion of two micelles with aggregation numbers Q_1 and Q_2 ($Q_2 \geq Q_1$) starts with the interpenetration of the micelle coronas.

We note that if micellar diffusion is treated as the diffusion of star polymers in a concentrated solution or melt, then it is rather slow: [29,34,35] $\tau_{\text{star}} \sim t_B^{\text{st}}P$, (where τ_B^{st} is the reptation time for one branch (B-block) to approach the core and $P \sim \exp[N_B]$ is the potential barrier for entering high polymer concentration region near the star core). The reason is the large time for B-blocks disentanglement. In the dilute or semidilute solutions, micellar diffusion can proceed quicker because only the tails of B-blocks outside the sphere of radius R_0 are strongly entangled. This means there is no need for entering dense region near micelle core for B-block disentanglement, and hence, there is no potential barrier. So, micellar diffusion can be regarded as a motion of a large sphere of radius R_0 surrounded by B-block tails in the region with the average polymer concentration c. The diffusion time is defined by the time required for the tail disentanglement only, τ_B.

The time for disentanglement of the B-block tail, τ_B, can be calculated in the following manner. Taking into account that the conformation of the B-block tail can be described as a chain of "concentration blobs"[27] of size $\xi = (cv)^{-3/4}v^{1/3}$ the motion of the tail to be disentangled is in fact reptation along the corresponding tube of blobs. The contour length of the tube is $L_{\text{pr}} \simeq (R_{\text{corona}} - R_0)^2/\xi$, where ξ plays the role of the step length of the primitive path. The diffusion coefficient for the chain of blobs is $D_b \simeq kT/N_{\text{blob}}\zeta_{\text{blob}} \simeq kT/\eta_s N_{\text{blob}}\xi$. The number of blobs in the tail is on the order of $N_{\text{blob}} \simeq N_B/n_{\text{bl}}$, where n_{bl} is the number of monomer units per blob,[27] $n_{\text{bl}} = (\xi/v^{1/3})^{1/\nu}$. Hence, for the diffusion coefficient we get

$$D_b \simeq \frac{kT}{\eta_s v^{1/3} N_B (cv)^{1/2}} \quad \text{(A7)}$$

The characteristic time for the B-block tail disentanglement and hence the time for the micellar diffusion is

$$\tau_{\text{dif}}^{\text{mic}} \simeq \tau_B \simeq \frac{{L_{\text{pr}}}^2}{D_b} = \frac{(R_{\text{corona}} - R_0)^4}{\xi^2}\frac{\eta_s v^{1/3}}{kT} N_B (cv)^{1/2} = \frac{\eta_s v}{kT} N_B^{17/5} Q_1^{4/5} (cv)^2 (1 - X')^4 \quad (\text{for } \nu = {}^3/_5,\ X' = R_0/R_{\text{corona}}) \quad \text{(A8)}$$

Therefore, the diffusion time increases with an increase of B-block length and concentration.

Corona Deformation. The next stage of micellar merging is penetration of the smaller micelle into the "internal" corona region (inside sphere of radius R_0) of the larger micelle. This process involves the reorganization of the "inner" corona regions for both micelles, which requires a decrease in solvent concentration and the redistribution of B-monomer units among the blobs with a decrease in blob size. The main conformational modifications concern the chains belonging to the interpenetration region of two micelles. The conformation

of the chains of blobs in this region changes in a manner similar to the electric field lines near charged spheres as they approach each other. For the most of the chains of blobs, the changes are manifested mainly in (cooperative) rotation around the micellar center accompanying by the blob compression.

The characteristic time for the corona deformation can be estimated using the analogy between the motion of the chain of blobs (inside the sphere of radius R_0 for larger micelle) and rotational motion of rod-like polymer chains in semidilute solutions.[29] The whole process can be split into two parts: rotation inside the original tube of blobs (the B-block conformation can be described as an almost radially oriented chain of blobs increasing in size as distance from the core increases[27]) and the tube relaxation. The angle through which a polymer chain can rotate without being hindered by other chains is $\varphi \simeq \xi/R_0 = Q_2^{-1/2}$ (ξ is the blob size at the distance R_0 from the core). To proceed further, the tail of the chain should be disengaged. The characteristic time for tail disentanglement is τ_B (with $Q = Q_2$), which plays the role of the tube relaxation time. Hence, the characteristic time associated with the corona deformation can be defined as the inverse rotational diffusion constant[29]

$$\tau_{def}^{mic} \simeq \frac{1}{D_{rot}} = \frac{\tau_B}{\varphi^2} = \frac{\eta_s v}{kT} N_B^{17/5} Q_2^{9/5} (cv)^2 (1 - X)^4 \quad \text{for } Q < (cv)^{5/2} N_B^2 \quad \text{(A9)}$$

The time for corona deformation, $\tau_{def}^{mic} \simeq Q\tau_B$, is evidently longer than that for micellar diffusion, $\tau_{dif}^{mic} \simeq \tau_B$.

When the aggregation number of merging micelles is relatively small, corona deformation can proceed somewhat quicker, because polymer concentration in the corona region is smaller and hence so is the degree of entanglement. We can assume that chain entanglement occurs mainly between the tails of B-blocks belonging to different micelles while they are merging. To estimate characteristic time for corona deformation, we still can apply the ratio $\tau_{def}^{mic} \simeq \tau_B/\varphi^2$, but now, τ_B is the time for a tail disentanglement of the smaller micelle:

$$\tau_{def}^{mic} \simeq \frac{\tau_B}{\varphi^2} = \frac{\eta_s v}{kT} N_B^{17/5} Q_1^{4/5} Q_2 (cv)^2 (1 - X)^4 \quad \text{(A10)}$$

For micelles with aggregation number $Q > (cv)^{5/2} N_B^2$, the whole process of corona merging consists of only corona deformation (unless Q_1 is very small, which we will consider below). The characteristic angle for rotation is on the order of $\varphi^* \simeq \xi_{corona}/R_{corona}$ (where $\xi_{corona} = N_B^{3/5} Q^{-3/10} v^{1/3}$ is the blob size at $r = R_{corona}$). Tube relaxation time can be estimated as disentanglement time for B-block $\tau_B^* = (n_s v/kT) N_B^{9/5} Q^{8/5}$, which can be calculated in a manner similar to τ_B with replacement of ξ by ξ_{corona} and R_0 by R_{core}. Then, the characteristic time for corona merging is on the order of

$$\tau_{def}^{mic} \simeq \frac{\tau_B^*}{\varphi^{*2}} \simeq \frac{\eta_s v}{kT} N_B^{9/5} Q_2^{13/5} \quad \text{for } Q > (cv)^{5/2} N_B^2 \quad \text{(A11)}$$

If the aggregation number of one of the micelles is much smaller than that for the other, i.e., $Q_1 \ll Q_2$, micelle fusion proceeds by diffusion of the smaller micelle through the corona of the larger micelle. The characteristic diffusion time can be estimated by using eq A8 and assuming that the motion occurs in the medium with polymer concentration equal to the average concentration inside the corona of the larger micelle, c_{corona}. As a result we get

$$\tau_{dif} \simeq \frac{\eta_s v}{kT} N_B^{9/5} Q_2^{4/5} Q_1^{4/5} \quad \text{for } Q_1 \ll Q_2 \quad \text{(A12)}$$

Core Merging. The final stage of micellar merging is penetration of A-blocks of the smaller micelle into the core region of the larger one to form a new core. This motion proceeds via collective reptation of A-blocks. The characteristic time for the process is on the order of τ_{core} (eq A6), with Q being the total aggregation number of a new micelle, i.e., $Q = Q_1 + Q_2$.

References and Notes

(1) Bedhar, B.; Edwards, K.; Almgren, M.; Tormod, S.; Tuzar, Z. *Makromol. Chem., Rapid Commun.* **1988**, *9*, 785.
(2) Halperin, A.; Alexander, S. *Macromolecules* **1989**, *22*, 2403.
(3) Prochazka, K.; Bednar, B.; Mukhtar, E.; Svoboda, P.; Trnena, J.; Almgren, M. *J. Phys. Chem.* **1991**, *95*, 4563.
(4) Pacovska, M.; Prochazka, K.; Tuzar, Z.; Munk, P. *Polymer* **1993**, *34*, 4585.
(5) Tian, M.; Qin, A.; Ramireddy, C.; Webber, S. E.; Munk, P.; Tuzar, Z.; Prochazka, K. *Langmuir* **1993**, *9*, 1741.
(6) Wang, Y.; Kausch, C. M.; Chun, M.; Quirk, R. P.; Mattice, L. W. *Macromolecules* **1995**, *28*, 904.
(7) Bednar, B.; Karasek, L.; Pokorny, J. *Polymer* **1996**, *37*, 5261.
(8) Honda, C.; Abe, Y.; Nose, T. *Macromolecules* **1996**, *29*, 6778.
(9) Haliloglu, T.; Mattice, W. L. In *Solvent and Self-Assembly of Polymers;* Webber, S. E., Ed.; Kluwer: Dortrecht, 1996.
(10) Haliloglu, T.; Bahar, I.; Erman, B.; Mattice, W. L. *Macromolecules* **1996**, *29*, 4764.
(11) Tuzar, Z. In *Solvent and Self-Assembly of Polymers;* Webber, S. E., Ed.; Kluwer: Dortrecht, 1996.
(12) Honda, C.; Hasegawa, Y.; Hirunuma, R.; Nose, T. *Macromolecules* **1994**, *27*, 7660.
(13) Goldmints, I.; Holzwarth, J. F.; Smith, K. A.; Hatton, T. A. *Langmuir* **1997**, *13*, 6130.
(14) Michels, B.; Waton, G.; Zana, R. *Langmuir* **1997**, *13*, 3111.
(15) Esselink, F. J.; Dormidontova, E.; Hadziioannou, G. *Macromolecules* **1998**, *31*, 2925.
(16) Esselink, F. J.; Dormidontova, E.; Hadziioannou, G. *Macromolecules* **1998**, *31*, 4873.
(17) Aniansson, E. A. G.; Wall, S. N. *J. Phys. Chem.* **1974**, *78*, 1024.
(18) Aniansson, E. A. G.; Wall, S. N. *J. Phys. Chem.* **1975**, *79*, 857.
(19) Aniansson, E. A. G.; Wall, S. N.; Almgren, M.; Hoffmann, H.; Kielmann, I.; Ulbricht, W.; Zana, R.; Lang, J.; Tondre, C. *J. Phys. Chem.* **1976**, *80*, 905.
(20) Lessner, E.; Teubner, M.; Kahlweit, M. *J. Phys. Chem.* **1981**, *85*, 1529, 3167.
(21) Kahlweit, M. *J. Colloid Interface Sci.* **1982**, *90*, 92.
(22) Shusharina, N. P.; Saphonov, M. V.; Nyrkova, I. A.; Khalatur, P. G.; Khokhlov, A. R. *Ber. Bunsen-Ges. Phys. Chem.* **1996**, 100, 857.
(23) Halperin, A. *Macromolecules* **1987**, *20*, 2943.
(24) Birshtein, T. M.; Zhulina, E. B. *Polymer* **1989**, *30*, 170.
(25) Leibler, L.; Orland, H.; Wheeler J. C. *J. Chem. Phys.* **1983**, *79*, 3550.
(26) Kramers, H. A. *Physica* **1940**, *7*, 284.
(27) Daoud, M.; Cotton, J. P. *J. Phys.* **1982**, *43*, 531.
(28) Esselink, F. J; Semenov, A. N.; ten Brinke, G.; Hadziioannou, G.; Oostergetel, G. T. *Macromolecules* **1995**, *28*, 3479.
(29) Doi, M.; Edvards, S. F *The Theory of Polymer Dynamics;* Oxford University Press: New York, 1986.
(30) De Gennes, P. G. *Macromolecules* **1976**, *9*, 587.
(31) Klein, J. *Macromolecules* **1978**, *11*, 852.
(32) Marrucci, G. *J. Polym. Sci. Phys. Ed.* **1985**, *23*, 159.
(33) Daoud, M.; De Gennes, P. G. *J. Polym. Sci. Phys. Ed.* **1979**, *17*, 1971.
(34) De Gennes, P. G. *J. Phys.* **1975**, *36*, 1199.
(35) Pearson, D. S.; Helfand, E. *Macromolecules* **1984**, *17*, 888.

MA9809029